A Utility Transmission System RAS That Uses Systemwide Measurements to Detect Generation Loss

Abdulaziz Faisal A. A. Talfat
KAHRAMAA

Aaron Esparza, Jerin Monzi Mathew, Muthuraman Shanmugam, and Héctor J. Altuve Ferrer
Schweitzer Engineering Laboratories, Inc.

Presented at the
51st Annual Western Protective Relay Conference
Spokane, Washington
October 22–24, 2024

A Utility Transmission System RAS That Uses Systemwide Measurements to Detect Generation Loss

Abdulaziz Faisal A. A. Talfat, *KAHRAMAA*
Aaron Esparza, Jerin Monzi Mathew, Muthuraman Shanmugam, and Héctor J. Altuve Ferrer,
Schweitzer Engineering Laboratories, Inc.

***Abstract*—The Qatar General Electricity and Water Corporation utility (KAHRAMAA) imports power from multiple independent power producers (IPPs). The KAHRAMAA system connects via two 400 kV tie lines to the transmission network operated by the Gulf Cooperation Council Interconnection Authority (GCCIA) that interconnects the power systems of six GCC countries. Power system studies performed by GCCIA in 2020 and 2021 showed that the loss of generation in the KAHRAMAA power system caused tripping of both tie lines and separation of the KAHRAMAA power system from the GCCIA network. The authors describe the remedial action scheme (RAS) designed to detect generation loss and perform countrywide adaptive load shedding when required. In this project, we had no access to local generator measurements and breaker status information. We implemented a loss-of-generation detection logic based on wide-area measurements. We also describe the cybersecure communications network developed applying software-defined networking (SDN) technology. Finally, we report the results of the RAS factory acceptance testing using a hardware-in-the-loop environment based on real-time digital simulators.**

I. Introduction

The Qatar General Electricity and Water Corporation utility (KAHRAMAA, referred to as "the utility" throughout) manages the country's transmission and distribution system. It imports power from multiple independent power producers (IPPs). The country's total power generation is 8,612 MW; seven IPPs generate 8,421 MW.

Qatar is a member of the Gulf Cooperation Council Interconnection Authority (GCCIA), which manages the transmission network that interconnects the power systems of six GCC countries, as shown in Fig. 1. The utility power system connects to the GCCIA network through two 400 kV tie lines (Tie Line 41 and Tie Line 42) at the interconnection substation. During normal operating scenarios, the total active power flow on Tie Line 41 and Tie Line 42 fluctuates in the +/−20 MW range.

The protection schemes of Tie Line 41 and Tie Line 42 include the following:

- An out-of-step tripping (OOST) scheme that trips the tie lines to separate the utility power system from the GCCIA system during unstable power swings.
- A thermal protection scheme that trips the tie lines for overload conditions.

Fig. 1. The GCCIA network interconnects the power systems of six GCC countries.

Power system studies performed by GCCIA in 2020 and 2021 showed that a sudden, large generation loss in the utility system caused unstable power swings in Tie Line 41 and Tie Line 42. As a result, the OOST scheme trips these lines. The loss of these tie lines may also cause tripping of tie lines that interconnect the power systems of other countries to the GCCIA network.

The authors performed additional power system studies. We found that the sudden loss of more than 1,800 MW of generation (more than 20 percent of maximum demand) in the utility system caused unstable power swings in Tie Line 41 and Tie Line 42. We also found that shedding load in less than 400 ms prevented these unstable oscillations.

The utility system had a wide-area underfrequency load-shedding scheme that provided frequency stability in case of generation loss. However, this scheme was too slow to prevent the OOST scheme from tripping Tie Line 41 and Tie Line 42. Therefore, GCCIA recommended implementing a countrywide remedial action scheme (RAS) in the utility system to prevent Tie Line 41 and Tie Line 42 from tripping on power swings or overloading conditions.

In this paper, the authors describe the RAS that was designed, tested, and commissioned to prevent undesired tie-line tripping. In this project, we had no access to local generator

measurements and breaker information, so we implemented a novel logic based on wide-area measurements.

One scheme (RAS 1) detects sudden, large generation loss and performs fast, adaptive load shedding to prevent the OOST scheme from tripping the tie lines. Another scheme (RAS 2) detects slow generation loss and performs adaptive load shedding to prevent tie-line thermal protection operation.

We also describe the cybersecure communications network with four rings developed by applying software-defined networking (SDN) technology.

Finally, we report the results of the RAS factory acceptance tests (FATs) using a hardware-in-the-loop environment based on real-time digital simulators (RTDSs).

II. RAS System Architecture

The RAS system covers 53 substations, including 10 substations receiving feeders from IPP stations (generation-receiving substations), 42 load substations (load-shedding substations), and the GCCIA interconnection substation.

Fig. 2 shows the RAS overall system architecture, which comprises redundant front-end processors (FEPs), redundant RAS controllers (RACs), redundant HMI gateways (GTWs), remote substation input/output (I/O) modules, SDN switches (not shown in the figure), a central computing platform, and an HMI.

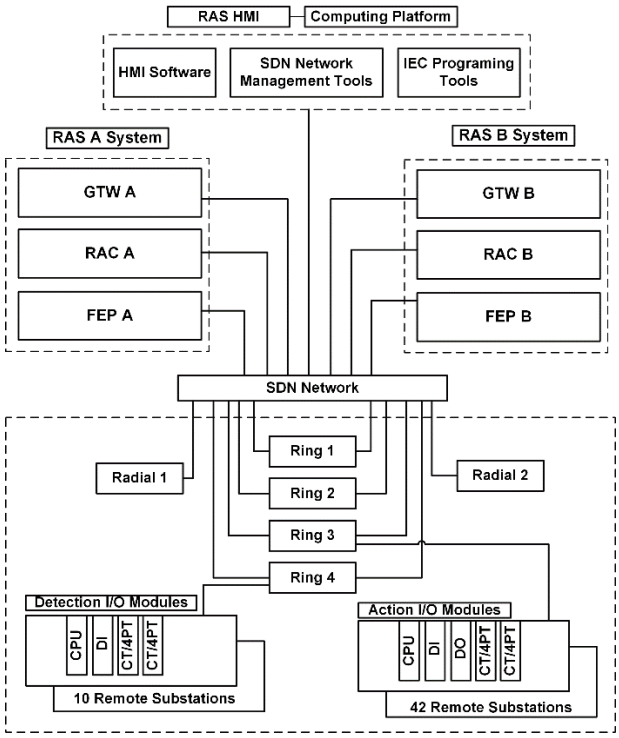

Fig. 2. RAS system architecture.

The RAS communications architecture is an SDN-based fiber-optic network that consists of four rings and two radial connections.

The remote substation I/O modules are placed in all 53 substations. These I/O modules are distributed among the four rings and the two radial connections. The I/O modules fall into two main categories:

- Detection I/O modules in the 10 generation-receiving substations.
- Action I/O modules in the 42 load-shedding substations.

Remote substation Detection I/O modules have digital input (DI) cards for monitoring breaker status and multiple current transformer (CT) and voltage transformer (VT) cards to obtain the necessary analog data from the CTs and VTs associated with the breakers monitored at each substation. Remote substation Action I/O modules have digital output (DO) cards for load shedding, in addition to DI, CT, and VT cards.

Remote substation I/O modules send analog and digital data using the Network Global Variable List (NGVL) protocol to the FEPs. The FEPs collect the data from the I/O modules, and then group, encapsulate, and segregate data based on speed. After segregation, the FEPs send the data to the RACs using the NGVL protocol for logic processing.

The RACs collect all the raw data from the FEPs and process them through a data conditioning filter to smooth out the continuously varying analog data and to identify breaker and metering alarms. After processing data, the RACs arm and execute the two main RAS algorithms described in Section III. The RACs perform logic calculations in subcycle processing intervals on the real-time measurements received from the field. Based on the load to shed values determined by the RAS algorithms and the load-shedding priorities set by the operator in the HMI, the RACs select loads to shed at every processing cycle. Then, the RACs send load-shedding commands to the FEPs, which in turn send these commands to the Action I/O Modules of the remote load-shedding substations.

The GTWs collect data from the RACs for HMI signaling. They also allow the HMI to send set points to the RACs.

The HMI performs comprehensive RAS monitoring. It provides detailed contingency summary screens for the two redundant systems. Other screens show load status, alarm status, network status, Sequence of Events (SOE), and event records.

The RAS has a dual-redundant architecture. Both RACs receive data, perform calculations, and independently initiate load-shedding actions. This approach is necessary because the inherent delay of traditional hot standby systems can exceed the permitted time budget, compromising system reliability. However, dual-primary redundancy poses a challenge: when a communications loss occurs, the two RACs may process different analog or digital values, leading to different calculation results and incorrect load shedding.

To address this, the RACs use a data quality index (DQI) to determine the RAC that will serve as a primary controller. Each RAC calculates the DQI based on the operational and communications status data for all field devices. The RACs assign different quality weights to the field devices based on the criticality of the information they provide. For instance, a FEP receives a higher weight than a general field device because of its potential impact on multiple devices. The resulting DQI is a weighted average of individual device DQI values.

The RAC with the highest DQI becomes the primary controller and replaces the output of the other controller. The

RACs dynamically determine this primary-secondary relationship in each processing cycle based on the comparison of the DQI values. By replacing the output of the secondary controller with that of the primary controller, only one set of load-shedding commands is transmitted to the FEPs, ensuring system consistency and preventing unintended operations.

III. RAS Logic Design

We performed a contingency analysis of the utility power system using modern simulation tools under various operation conditions. We studied the effect on Tie Line 41 and Tie Line 42 of the sudden or slow loss of IPPs. We determined the IPP losses that would either cause an unstable power swing or an overload condition on the tie lines.

We found that fast load shedding avoids unstable power swings and prevents the OOST scheme from tripping the tie lines on this condition. Similarly, slower load shedding prevents tie-line overloading and avoids thermal tripping of these lines.

Based on these results, we designed a RAS logic that reliably identifies these contingencies for diverse operating conditions. Given the lack of access to local generator measurements and breaker information, the RAS logic uses other measurements. We designed the following RAS functions:

- RAS 1: Fast load shedding for sudden generation loss.
- RAS 2: Load shedding for slow generation loss.

A. RAS 1: Fast Load Shedding for Sudden Generation Loss

Our studies showed that the sudden loss of any of the four largest IPPs has the potential to cause an unstable power swing on Tie Line 41 and Tie Line 42. The capacity of each of these IPPs falls in the 1,800 to 2,650 MW range. Our studies also showed that shedding load in less than 400 ms avoids unstable power swings and prevents the OOST scheme from tripping the tie lines. The utility selected 300 ms as the target RAS minimum load-shedding time.

Fig. 3 shows the RAS 1 activation logic. This activation logic considers additional factors (not shown in the figure), such as HMI enable and disable commands, contingency reset commands, and timers, to provide security.

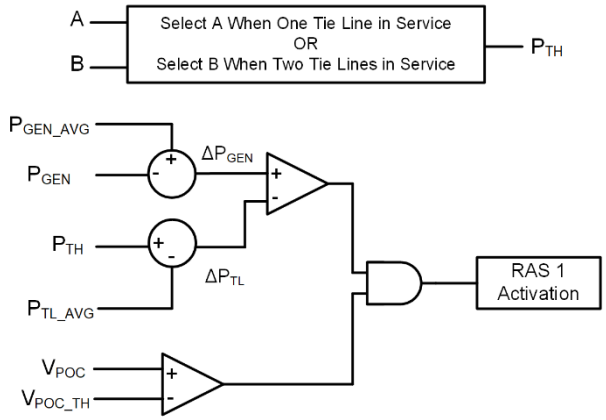

Fig. 3. RAS 1 activation logic.

The logic uses power measurements to detect unstable power swings in the tie lines and voltage measurements to prevent activation for faults.

- Unstable power swing detection: The RAS 1 activation logic compares the power generation loss in the utility power system with the change of power flowing through Tie Line 41 and Tie Line 42. For a sudden loss of any of the four largest IPPs, power generation drops fast and the tie-line power flow changes more slowly because of the large inertia of the GCCIA system.
- Security during faults: The RAS 1 activation logic compares the voltage measured at the generation-receiving substations with a threshold.

Fig. 3 shows the following variables and constants:

- P_{GEN} is the sum of the active power values measured on each in-service feeder line connecting the IPPs to the utility substations.
- P_{GEN_AVG} is the P_{GEN} average value. The controller calculates this value in each time step using a four-second data window.
- $\Delta P_{GEN} = P_{GEN\_AVG} - P_{GEN}$.
- P_{TL_AVG} is the P_{TL} average value, where P_{TL} is the sum of the active power values measured on Tie Line 41 and Tie Line 42. The controller calculates this value in each time step using a four-second data window.
- $\Delta P_{TL} = P_{TH} - P_{TL\_AVG}$.
- P_{TH} is an automatically selected tie-line power threshold value that depends on the lines in service. For one line in service, P_{TH} = A; for two lines in service, P_{TH} = B. A and B are user-defined settings.
- V_{POC} is the voltage measured at the point of common coupling of each IPP (the utility substation-side terminals of IPP-connecting lines). The controller compares V_{POC} with a threshold value V_{POC_TH}, which is a user-defined setting.

As shown in Fig. 3, the RAS 1 activation logic asserts when ΔP_{GEN} is greater than ΔP_{TL} and V_{POC} is greater than V_{POC_TH}.

Fig. 4 illustrates the RAS 1 process to calculate the amount of load to shed. The controller performs this calculation in parallel with the execution of the RAS 1 activation logic.

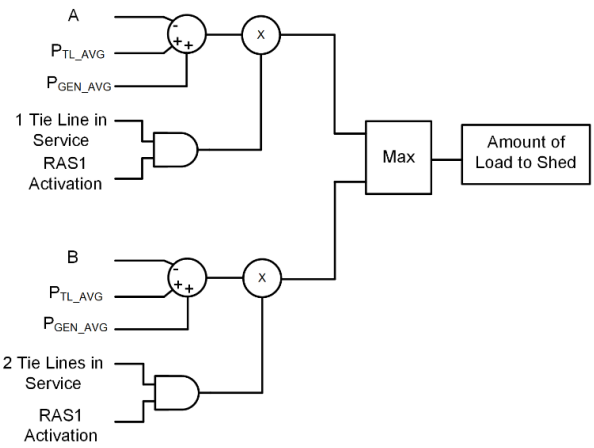

Fig. 4. RAS 1 calculation of load required to shed.

The RAS 1 logic calculates the sum of the average values of the IPP-generated power (P_{GEN_AVG}) and the tie-line transfer power (P_{TL_AVG}). When one tie line is in service, the logic subtracts the A power threshold value from the average value sum; when two tie lines are in service, the logic subtracts the B power threshold value from the average value sum. Then, the logic selects the maximum of the two values as the amount of load to shed.

B. RAS 2: Load Shedding for Slow Generation Loss

Our studies showed that certain slow or partial generation loss scenarios lead to an overload condition on Tie Line 41 and/or Tie Line 42 without causing an unstable power swing in these lines. The tie-line power transfer may reach the maximum power transfer limit (MPTL) set by GCCIA. In addition, the tie-line current may reach the line thermal limit and cause overload protection tripping. Our studies also showed that shedding load in the utility system prevents violating the tie-line MPTL and thermal limits and avoids overload protection tripping.

Fig. 5 shows the RAS 2 activation logic. This activation logic considers additional factors (not shown in the figure) to provide security.

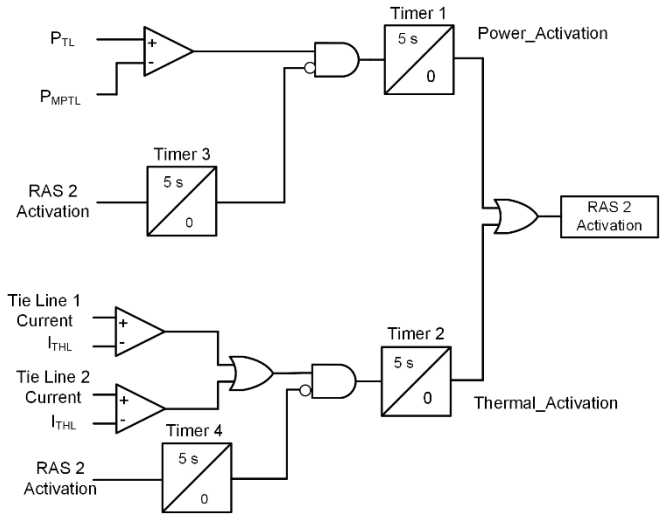

Fig. 5. RAS 2 activation logic.

The logic uses power measurements to detect tie-line MPTL violations and current measurements to detect tie-line thermal limit violations.

- Tie-line MPTL violation detection: The RAS 2 activation logic compares the active power value measured on the tie lines (P_{TL}) with the MPTL set by GCCIA (P_{MPTL}).
- Tie-line thermal limit violation detection: The RAS 2 activation logic compares the current measured on the tie lines with the current thermal limit (I_{THL}).

As shown in Fig. 5, the RAS 2 activation logic asserts when P_{TL} is greater than P_{MPTL} for 5 seconds (Timer 1 pickup setting), or either Tie Line 41 or Tie Line 42 current is greater than I_{THL} for 5 seconds (Timer 2 pickup setting). The five-second timer pickup adds security to ensure that the limit violation detected is not a transient condition. Furthermore, the timers are set for RAS 2 to operate faster than the tie-line overload protection.

The tie-line overload protection uses an IEC inverse curve with a pickup setting of 3,140 A primary. With these settings, overload protection trips in 30 seconds for the loss of the largest IPP in the utility system.

In addition, the RAS 2 activation logic opens a five-second time window (Timer 3 and Timer 4) for load shedding to take place. If the Power_Activation or Thermal_Activation bits are asserted when the timers expire, the timers reset the RAS 2 activation logic via the AND gates. This way, RAS 2 is ready to start a new load-shedding cycle if still required.

Fig. 6 illustrates the RAS 2 process to calculate the amount of load to shed. The controller performs this calculation in parallel with the execution of the RAS 2 activation logic.

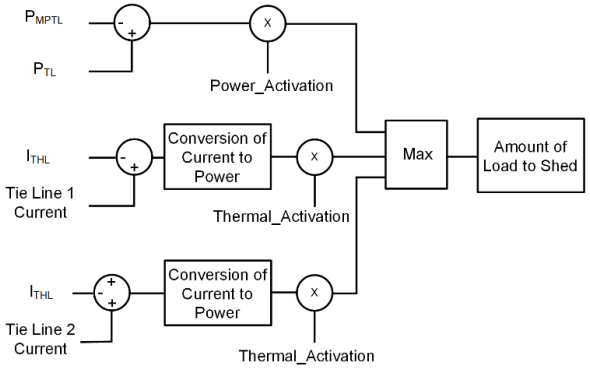

Fig. 6. RAS 2 calculation of load required to shed.

The RAS 2 logic calculates the value of $P_{TL} - P_{MPTL}$ and multiplies this value by the Power_Activation bit. Similarly, the logic subtracts I_{THL} from the Tie Line 41 and Tie Line 42 currents and converts the resulting current values to power values. Then, the logic multiplies these values by the Thermal_Activation bit. Finally, the logic selects the maximum of the three values as the amount of load to shed. The logic outputs a value of the required load to shed when the Power_Activation bit and/or the Thermal_Activation bit assert.

IV. RAS Communications Network Design

The 53 substations covered by the RAS project are spread across the utility power system. The communications network needed to interconnect all these substations requires a communications technology that is purpose-engineered, deterministic, and cybersecure [1].

The utility power system has more than 200 substations that are interconnected by a meshed fiber-optic network. We used the existing dark fibers to develop the RAS fiber-optic network backbone.

Using the dark fiber network drawing, we determined the lengths of the optical fibers between all pairs of substations. We found the longest distance to be 40 km. As a result, we decided to use single-mode optical fibers in the RAS communications network. Since most RAS substations are not adjacent in the utility fiber-optic network, many links between RAS substations include passive connections via fiber-optic patch panels (FOPPs).

These passive connections increase the overall attenuation in the fiber-optic link. The maximum link loss shall not exceed

18 dB. We calculated the link loss to optimize the design before system implementation in the field. We used the following equation to calculate the link loss in dB:

$$\text{Link Loss} = (F_{LNGT} \bullet F_{LOSS}) + (S_{LOSS} \bullet N_S) + (C_{LOSS} \bullet N_C) + M_{SAF}$$

where:

F_{LNGT} is the fiber-optic link length in km.

F_{LOSS} is the optical fiber attenuation in dB per km (typically 0.3 dB).

S_{LOSS} is the loss per splice (typically 0.1 dB).

N_S is the number of splices.

C_{LOSS} is the loss per connector (typically 0.75 dB).

N_C is the number of connectors.

M_{SAF} is the safety margin (typically 4.5 dB).

In the communications network design, we selected 30 km as the maximum fiber-optic link length to keep link loss within allowable limits.

Fig. 7 depicts an example of a fiber-optic ring interconnection between substations. The ring connects with two different centralized RAS switches (SWs). The switches located in generation-receiving substations are called Detection Switches, and the switches located in load-shedding substations are called Action Switches. The figure also shows the FOPPs located in some substations not covered by the RAS.

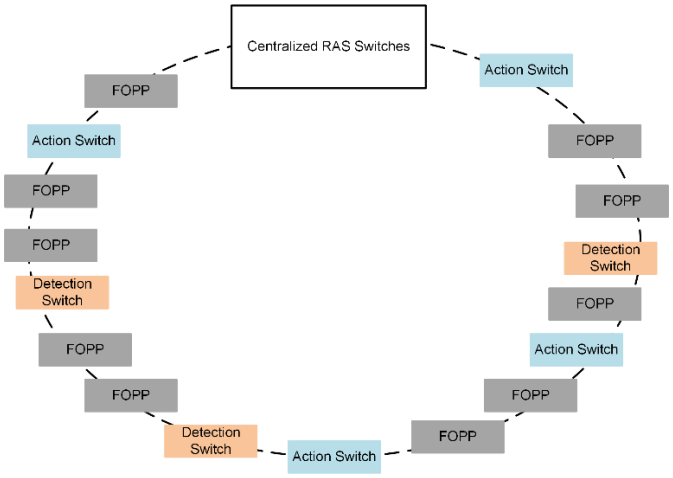

Fig. 7. Example of a fiber-optic ring connecting several substations.

Fig. 8 depicts a simplified RAS SDN communications network diagram. The distance and operation time limitations require a network topology with four rings. Each ring connects with two switches in the centralized switch panel. Each ring interconnects switches located in generation-receiving and load-shedding substations and FOPPs located in other substations.

We selected a network ladder topology to reduce the length of the optical fibers and minimize the use of passive connectors. We limited the number of RAS substations in each ring to 15. This arrangement reduces the number of switches to lose to 15 in case of two optical fibers failing in the same ring.

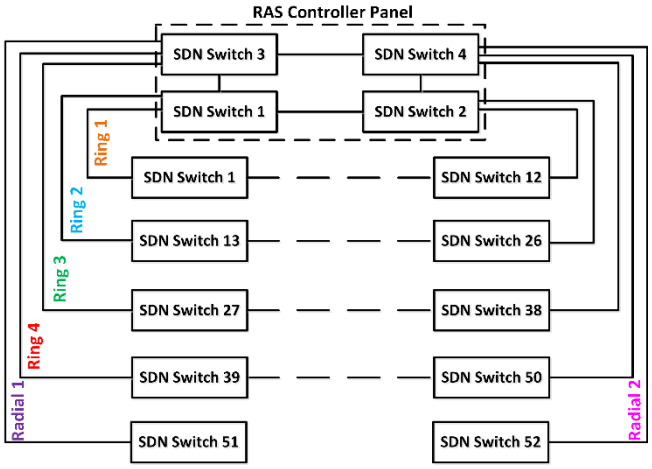

Fig. 8. Simplified RAS SDN network diagram.

SDN Switches 1, 2, 3, and 4, located in the RAS main controller panel, facilitate data exchange with the ring switches. SDN Switches 1 and 2 connect to Rings 1 and 2 and only exchange signals with the RACs. SDN Switches 3 and 4 connect to Rings 3 and 4 and only exchange signals with the RACs. This arrangement prevents unwanted data flow between rings.

The ring switches collect and aggregate critical data from the generation-receiving substations and the tie-line substation, and then send the data to the centralized RACs. They also transfer tripping commands from the RACs to the load-shedding substations.

We implemented a multicentric ladder topology to optimize bandwidth utilization in each ring and enhance network robustness. This configuration ensures resilience by preventing a single device failure from causing a complete loss of RAS data. For example, a malfunction of the RAS controller panel SDN Switch 1, connected to Rings 1 and 2, would not result in the total disruption of these rings, as they can continue sending and receiving data through Switch 2. No data exchange occurs between rings. In case of a total ring loss, the RAS selects loads from substations connected to the remaining rings, which ensures dependability.

We selected operational technology (OT) SDN technology because of its advantages compared to traditional communications network technology [2]. SDN technology has the following benefits:

- Inherent cybersecurity by applying deny-by-default technology.
- Fast failover by proactively engineering primary and backup paths. Does not require network reconfiguration.
- Easy configuration using the zero-touch deployment (ZTD) tool.

Cybersecurity was one of the primary considerations when designing the RAS network because the RAS performs load-shedding actions in 42 substations. Any unintentional load

circuit tripping of a load-shedding substation because of a cyberattack can affect many customers, as occurred in the 2015 cyberattack on the Ukrainian power system [3]. SDN switches are deny-by-default Ethernet switches; they only allow configured communications in the network as per a flow configuration table.

In addition, because all the network communications are pre-engineered, including the primary and backup communications paths, the SDN network can failover to a backup path within 100 µs, compared to the 15 ms failover time of an Ethernet network using the rapid spanning tree protocol (RSTP) [2].

Fig. 9 illustrates a simplified diagram of SDN data flow in the RAS communications network. The figure shows the primary and backup path selection process that the SDN switches follow to dependably perform data exchange between the RAC substations. For example, in the event of an optical fiber failure between Switches 3 and 4, the SDN switches automatically transfer the data path to a preprogrammed backup path within 100 µs to ensure uninterrupted information exchange in the RAS.

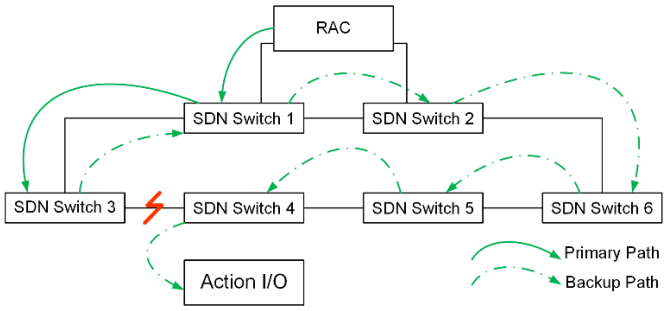

Fig. 9. Simplified diagram of SDN data flow in the RAS network.

The ZTD tool simplifies the SDN network configuration process. Configuring an SDN network only requires a network architecture drawing and a data flow diagram in a format compatible with the ZTD tool [4]. The information the ZTD tool requires to configure the SDN network includes device types and protocol information, device IP addresses, and network interconnection information.

The control plane of the SDN network resides in the SDN controller software; the SDN switch software contains only data planes [2]. This arrangement allows a user to centrally manage the SDN network through the SDN controller software. The SDN controller also performs comprehensive monitoring of the communications network, including real-time communications link monitoring, SDN switch health monitoring, SOE monitoring, and monitoring of all configured flow rules.

Centrally managing the SDN switches also allows all firmware upgrades and configuration updates of the SDN switches to be performed from a central location. SDN technology offers ease of maintenance to the users whose substations are unmanned.

V. RAS Hardware-in-the-Loop Testing

We performed FATs in a hardware-in-the-loop test environment to validate the RAS logic. We linked the RACs and associated equipment with an RTDS.

We validated the RTDS model by comparing simulation results with those obtained from power system studies using a complete Power System Simulator for Engineering model of the utility system. We also compared RTDS simulation results with real contingency events provided by the utility. The validation process showed that the RTDS model faithfully represents the power system and ensures that FAT results are reliable.

Fig. 10 shows the FAT network architecture. We used a reduced system with six generation-receiving substations and six load-shedding substations spread across four rings and two radial connections in the communications network. Action I/Os and Detection I/Os receive field information from the RTDS. The FEPs receive information for all remaining substations directly from the RTDS. Action I/Os and FEPs send load-shedding commands to the RTDS when the RACs make a remedial action decision.

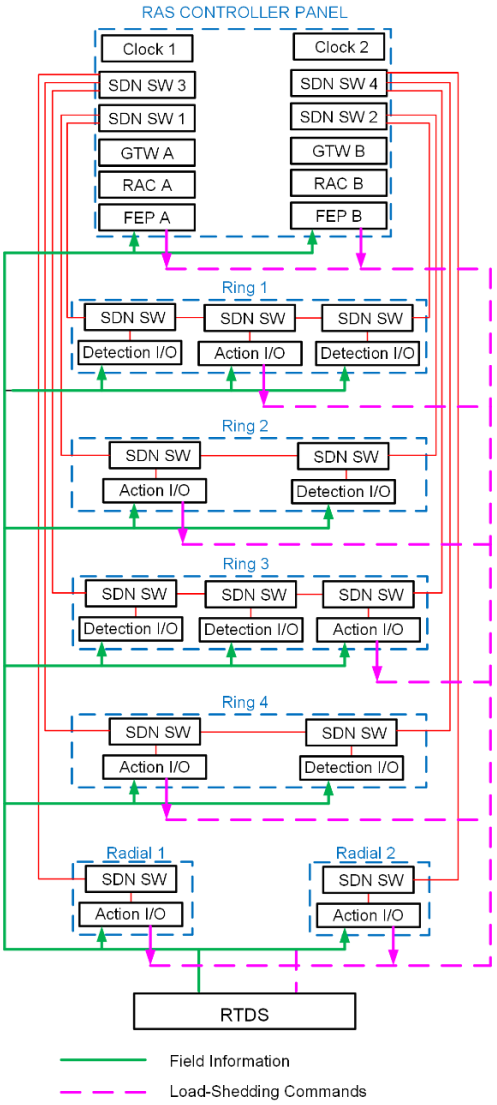

Fig. 10. FAT network architecture.

This configuration allows the following validations to be performed:

- RAS logic performance (activation when required, no activation when not required, and correct load-shedding operations).
- Communications equipment performance.
- Total RAS operating time (the time from contingency detection to load-shedding execution).
- HMI performance.

We conducted many tests to verify the performance of RAS 1 and RAS 2 logic.

As an example of a RAS 1 logic test, Fig. 11 and Fig. 12 show the response of the utility power system for a major contingency (the sudden loss of the largest IPP of the country). The total power loss in the system is 2,220 MW. The predisturbance power transfer through the tie lines equals zero.

The figures show the active power measured on eight generation-receiving substations and on the tie lines (GCCIA_EQ_P). The power from the substation connected to the largest IPP drops suddenly to zero. The power of the other seven generation-receiving substations shows the typical oscillatory inertial responses of the IPPs to the disturbance. The tie-line power transfer increases to compensate for the generation loss, but this inertial response is slower because of the large inertia of the GCCIA interconnected system.

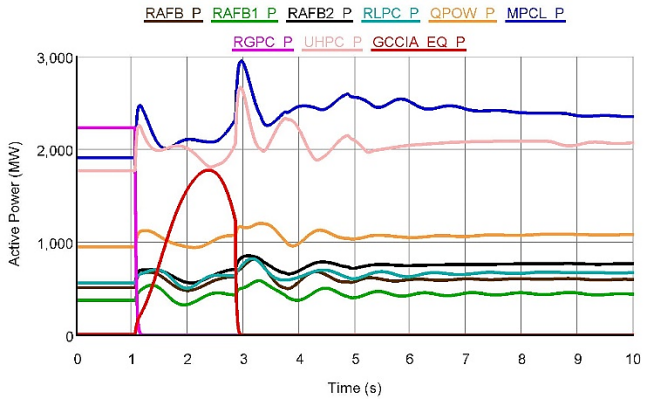

Fig. 11. Power system response to the sudden loss of a large IPP with RAS disabled.

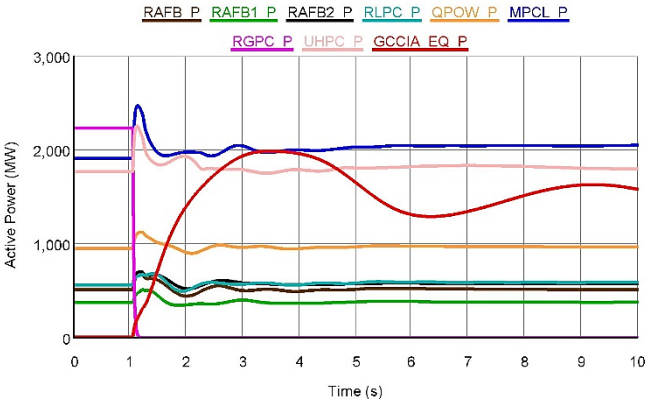

Fig. 12. Power system response to the sudden loss of a large IPP with RAS enabled.

When the RAS is disabled (see Fig. 11), the tie-line OOST scheme detects the unstable power swing and trips the tie lines two seconds after the disturbance starts. The tie-line transfer power (GCCIA_EQ_P) drops to zero.

When the RAS is enabled (see Fig. 12), it detects the contingency and sheds load in less than 100 ms. This load shedding prevents the unstable power swing. After some time, the tie-line power oscillations dampen out, and the interconnection between the utility system and the GCCIA system remains intact. For this event, the RAS selected to shed approximately 432 MW.

Fig. 13 shows the active and reactive power transfer through the tie lines and the power system frequency.

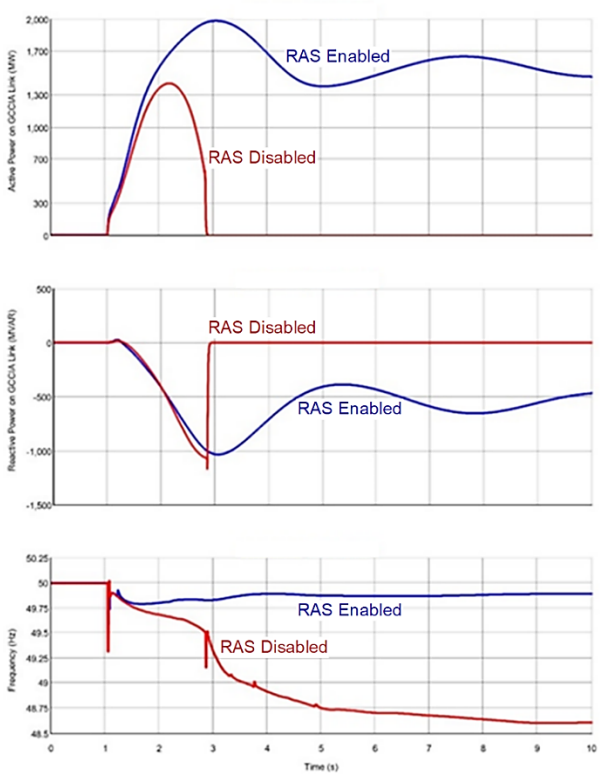

Fig. 13. Tie-line active and reactive power transfer and power system frequency for the cases with the RAS is disabled (red line) and enabled (blue line).

When the RAS is disabled, the tie-line active and reactive powers grow monotonically and then drop to zero when the OOST scheme trips the tie lines. The power system frequency drops to 48.54 Hz. The frequency stabilizes when three of the five steps of the underfrequency load-shedding scheme operate. Load shedding occurs at t = 3.16 s, t = 3.6 s, and t = 4.82 s. The total amount of load to shed is around 950 MW. This value is more than twice the 432 MW of load shed by the RAS when enabled.

When the RAS is enabled, it sheds load and the tie-line power swing is stable. The active and reactive power oscillations dampen out after some time. The power system frequency only drops to 49.75 Hz because of the high inertia of the GCCIA interconnected system.

The RAS 1 action provides two important results. First, the system maintains the interconnection closed (the main objective of RAS 1). Second, RAS 1 sheds less load than the load the underfrequency scheme would have shed if the RAS had been disabled.

Fig. 14 illustrates the OOST scheme performance during the event. The figure shows the power swing impedance trajectories measured by the tie-line OOST elements (green lines in the figure). The OOST elements use a double-blinder scheme for power swing detection. The blue lines in the figure represent the blinders with their actual settings. The external blinder settings are ± 50 ohms.

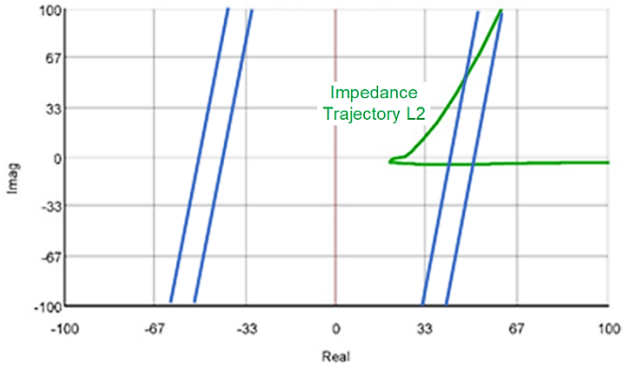

Fig. 14. Impedance trajectory for the sudden loss of a large IPP with RAS disabled.

When the RAS is disabled (see Fig. 14), the impedance trajectory crosses both right-side blinders and the OOST scheme trips. When the RAS is enabled (see Fig. 15), the impedance trajectory does not reach the external blinder because RAS 1 fast load shedding prevents the system from losing synchronism.

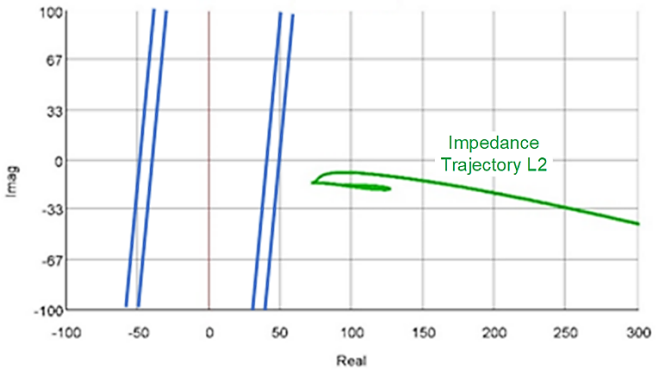

Fig. 15. Impedance trajectory for the sudden loss of a large IPP with RAS enabled.

We conducted many similar tests considering loss of other large IPPs for different power system operating conditions and states. We found that the RAS 1 operation avoided the OOST scheme tripping in all cases.

As an example of a RAS 2 logic test, we simulated a power loss of the largest IPP (for example, a failure in the gas supply system). The total generation loss occurred in approximately 60 seconds.

Fig. 16 shows the response of the power system for this slow generation loss condition. The figure shows the slow decrease of power from the substation connected to the IPP (trace labeled RGPC in the graph). The tie-line power transfer (GCCIA_EQ_P) increases to compensate for the generation loss and even becomes greater than the P_{MPTL_TH} value. RAS 2 triggers load shedding in approximately 15 seconds; the tie-line power transfer stabilizes and no thermal tie-line tripping occurs. The tie-line power transfer remains above P_{MPTL_TH} for only 5 seconds.

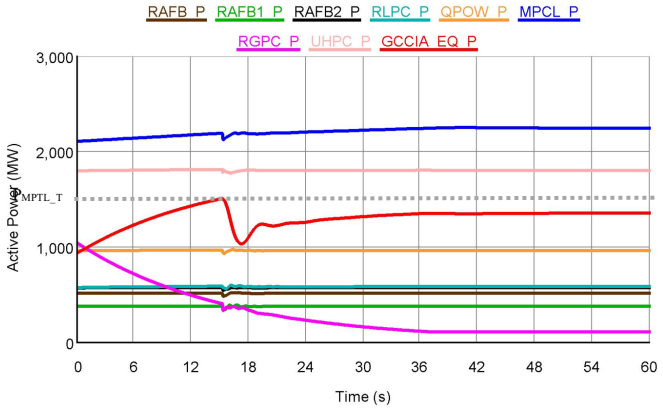

Fig. 16. Power system response to a slow generation loss condition.

Fig. 17 shows the active and reactive power transfer through the tie lines and the power system frequency. Active power increases, reactive power decreases, and frequency falls to 49.9 Hz. Load shedding occurs in approximately 15 seconds, and power transfers stabilize. Frequency grows by 0.02 Hz.

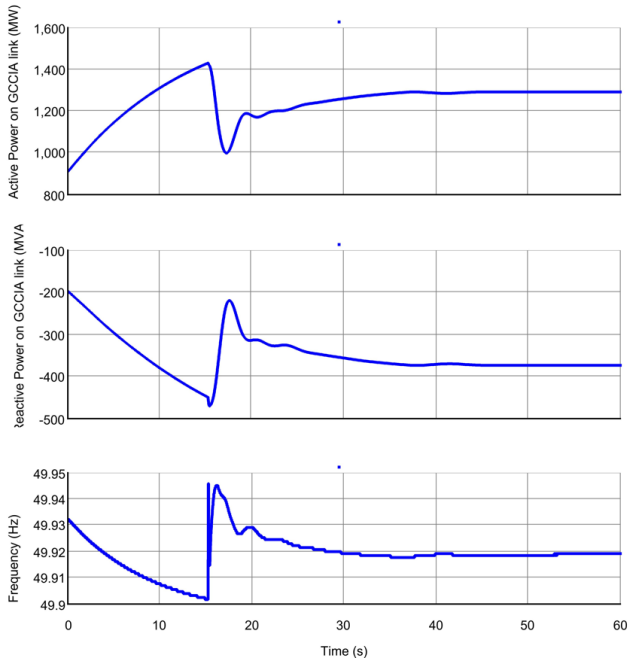

Fig. 17. Tie-line active and reactive power transfer and power system frequency for a slow generation loss condition.

Fig. 18 illustrates the OOST scheme performance during the event. As expected, the impedance trajectory remains far away from the blinders for this slow generation loss condition.

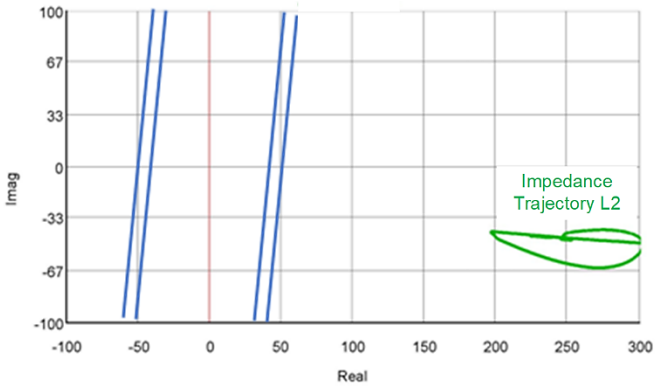

Fig. 18. Impedance trajectory for a slow generation loss condition.

We conducted many similar tests considering slow generation loss conditions of other IPPs for different power system operating conditions and states. We found that the RAS 2 operation avoided thermal line tripping in all cases.

VI. Conclusion

KAHRAMAA imports power from multiple IPPs. The utility system connects through two tie lines to the GCCIA interconnected power network. Power system studies performed by GCCIA showed that the loss of generation in the utility system causes tie-line tripping and separation of its power system from the GCCIA network.

Our own studies showed that the sudden generation loss of more than 1,800 MW in the utility system causes unstable power swings in the tie lines. We also found that shedding load in less than 400 ms prevents these unstable power swings.

We describe the RAS that we designed, tested, and commissioned to prevent undesired tie-line tripping. The RAS covers 53 substations, including 10 generation-receiving substations, 42 load-shedding substations, and the GCCIA interconnection substation. In this project, we had no access to local generator measurements and breaker information, so we implemented a novel logic based on wide-area measurements.

RAS 1 detects sudden, large generation loss and performs countrywide fast, adaptive load shedding to prevent the OOST scheme from tripping the tie lines. RAS 2 detects slow generation loss and performs countrywide adaptive load shedding to prevent operation of the tie-line thermal protection.

The RAS communications network has a ladder topology with four rings. Each ring connects with two switches in the centralized switch panel. Each ring interconnects switches located in generation-receiving and load-shedding substations and FOPPs located in other substations. We limited the number of RAS substations in each ring to 15 to reduce switch losses in case of optical fiber failures.

We selected SDN technology for the communications network. SDN networks are inherently cybersecure, provide fast failover actions, and are easy to configure.

We tested the RAS using a hardware-in-the loop system based on RTDSs. We conducted many tests simulating the sudden loss of large IPPs. We found that RAS 1 shed load in less than 100 ms and prevented the OOST scheme from tripping the tie lines in all cases. We also conducted many tests simulating IPP slow output power loss conditions. We found that RAS 2 operation avoided thermal line tripping in all cases.

VII. References

[1] S. Manson and D. Anderson, “Practical Cybersecurity for Protection and Control System Communications Networks,” presented at the 64th Annual Petroleum and Chemical Industry, Calgary, Canada, Sept. 2017.

[2] A. Kalra, D. Dolezilek, J. M. Mathew, R. Raju, R. Meine, and D. Pawar, “Using Software-Defined Networking to Build Modern, Secure IEC 61850-Based Substation Automation Systems,” proceedings of the 15th International Conference on Developments in Power System Protection (DPSP 2020), Liverpool, United Kingdom, March 2020.

[3] D. E. Whitehead, K. Owens, D. Gammel, and J. Smith, “Ukraine Cyber-Induced Power Outage: Analysis and Practical Mitigation Strategies,” proceedings of the 70th Annual Conference for Protective Relay Engineers (CPRE), College Station, TX, April 2017.

[4] D. Bordon, R. Meine, S. Dayabhai, and J. Dearien, “Case Study: Implementing a Zero-Touch Deployment Methodology Using SDN to Improve the Security, Reliability, and Engineering of Substation Automation Systems in Slovenia,” proceedings of the PAC World Conference 2023, Glasgow, United Kingdom, June 2023.

VIII. Acknowledgments

The authors thank Nabeel Nisam of Schweitzer Engineering Laboratories, Inc. (SEL) for his support during the RAS FAT. The authors also acknowledge the contribution of Rajkumar Raju, Karukkuvel Ayyanar, and Shakeel Mohamed of SEL during the RAS commissioning and field testing.

IX. Biographies

Abdulaziz Faisal A. A. Talfat is manager, Electricity Transmission Department, Qatar General Electricity and Water Corporation (KAHRAMAA), in Doha, Qatar. He has 11 years of experience: eight years working as an overhead line engineer and three years in managerial positions. He received the BSEE degree from Cardiff University, Wales, UK, in 2013. His areas of interest are the latest protection and switchgear developments, substation automation systems, overhead line networks, and digital substations.

Aaron Esparza is a project engineer in the special protection systems department of Schweitzer Engineering Laboratories, S.A. de C.V. (SEL) in Mexico. He received the ME and PhD degrees in electrical engineering from the Autonomous University of San Luis Potosí, San Luis Potosí, Mexico, in 2013 and 2018, respectively. His research interests are in power system digital modeling and simulations, wide-area protection, and control applications.

Jerin Monzi Mathew is a project engineer in the special protection systems group of Schweitzer Engineering Laboratories Middle East FZCO (SEL) Engineering Services (ES) in Dubai, United Arab Emirates. He started his career at SEL in 2017. He received his BE degree in electrical and electronics engineering from Anna University, Chennai, India. He also received a postgraduate diploma in subtransmission and distribution from the National Power Training Institute, Bangalore, India. His areas of interest are in power management systems, substation automation systems, digital secondary systems, and OT networks.

Muthuraman Shanmugam is the special protection systems manager of the Engineering Services Division of Schweitzer Engineering Laboratories Saudi Limited (SEL) in Saudi Arabia. He received the BE EE degree from Annamalai University. He has been employed at SEL since 2014 and has experience in designing and implementing control systems for utility and industrial customers.

Héctor J. Altuve Ferrer received his BSEE degree in 1969 from the Central University of Las Villas in Santa Clara, Cuba, and his PhD degree in 1981 from Kiev Polytechnic Institute in Kiev, Ukraine. From 1969 until 1993, Dr. Altuve served on the faculty of the Electrical Engineering School at the Central University of Las Villas. From 1993 to 2000, he served as professor of the Graduate Doctoral Program in the Mechanical and Electrical Engineering School at the Autonomous University of Nuevo León in Monterrey, Mexico. In 1999 through 2000, he was the Schweitzer Visiting Professor in the Department of Electrical and Computer Engineering at Washington State University. Dr. Altuve joined Schweitzer Engineering Laboratories, Inc. (SEL) in January 2001, where he is currently a distinguished engineer and dean of SEL University. He has authored and coauthored more than 100 technical papers and several books and holds four patents. His main research interests are in power system protection, control, and monitoring. Dr. Altuve is an IEEE life fellow.